ELSEVIER

Applied Catalysis A: General 185 (1999) 237–245

APPLIED CATALYSIS A: GENERAL

Decomposition of hydrogen peroxide in a catalytic fluidized-bed reactor

Shanshan Chou[1], Chihpin Huang *

Institute of Environmental Engineering, National Chiao Tung University, Hsinchu 30039, Taiwan

Received 25 September 1998; received in revised form 16 February 1999; accepted 6 May 1999

Abstract

The decomposition of H_2O_2 by a novel supported γ-FeOOH catalyst was performed in a continuous fluidized-bed reactor. This catalyst has been successfully used in the treatment of organic contaminants with H_2O_2 in our previous work. In this study, we attempted to determine the effects of pH, H_2O_2 concentration, and catalyst concentration on the decomposition of H_2O_2. An approach, we regarded this reactor as a continuous-flow stirred-tank reactor, was applied to investigate the kinetic behavior. At low H_2O_2 concentration, the decomposition rate of H_2O_2 was found to be proportional to both H_2O_2 and catalyst concentrations. At high H_2O_2 concentration, however, the rate decreased with the increasing H_2O_2 concentration. This can be explained by the substrate inhibition model. The large difference in the observed first-order rate constants under various pH values was also modeled. The model agreed well with the experimental results.

Keywords: Iron oxide; Hydrogen peroxide; Heterogeneous catalysis; Fluidized bed

1. Introduction

Hydrogen peroxide has been found to be useful in wastewater treatment [1,2] and in soil remediation [3,4]. It is a powerful oxidant for contaminants working either alone or in conjunction with a catalyst [4]. The most common homogeneous catalyst is ferrous iron. When combined with H_2O_2, it is well known as Fenton's reagent [5]; heterogeneous catalysts involve metal oxides, and supported metal oxides [6]. Recently, the application using iron oxide catalyst has been studied extensively [3,6–9]. Goethite, hematite, semicrystalline, and ferrihydrite have been used as catalysts to treat the organic contaminants [3,7,8]. In our previous work, we developed a novel supported γ-FeOOH catalyst and proved that it can effectively remove benzoic acid and 2,4,6-trichlorophenol [9]. All the results indicate that the removal of contaminants is related to the catalytic decomposition of H_2O_2 by iron oxide. Due to this important role, the catalytic decomposition of H_2O_2 deserves further investigation.

The continuous-flow stirred-tank reactor (CSTR) has been considered as the most attractive reactor for studying the kinetics of solid catalyzed reaction [10]. Most of the studies mentioned above, however, were performed in the batch mode. To prevent the catalyst from any damage due to mechanical mixing, we selected a fluidized-bed reactor (FBR) to conduct experiments. The performance in circulating FBR is similar to that in CSTR when the recycle ratio is large enough [10,11]; the method has been extensively applied in

* Corresponding author. Tel.: +886-3-5726463; fax: +886-3-5725958; e-mail: cphuang@green.ev.nctu.edu.tw

[1] Present address: Union Chemical Laboratories, Industrial Technology Research Institute, Hsinchu, Taiwan.

0926-860X/99/$ – see front matter
PII: S0926-860X(99)00140-4

Table 1
Properties of the catalyst

Parameters	Value
Iron content ($g\,kg^{-1}$)	135
Total surface concentration of iron[a] ($g\,kg^{-1}$)	95
Bulk density ($g\,cm^{-3}$)	1.11
Dry density ($g\,cm^{-3}$)	1.70
Average particle size (mm)	0.564
Specific surface area ($m^2\,g^{-1}$)	48.3
Surface site ($mole\,g^{-1}$)	5.89×10^{-4}
pK_{a1}	5.3
pK_{a2}	8.8
pH_{pzc}(point of zero charge)[b]	7.05

[a] Total surface concentration of iron on the catalyst = iron content of catalyst − iron content of support.
[b] $pH_{pzc} = (pK_{a1} + pK_{a2})/2$.

heterogeneous catalysis due to its high efficiency in mass transfer [10].

In this study, we attempted to evaluate the performance of the continuous circulating FBR with the supported γ-FeOOH catalyst. The effects of pH, H_2O_2 concentration and catalyst concentration on the decomposition of H_2O_2 were studied.

2. Experimental

2.1. Catalyst preparation

A novel catalyst, iron oxide on a brick grain support, was developed in the following manner [12]. The brick grains were packed in a 6.1 l (6.8 cm ϕ × 170 cm-H) FBR as carriers. To maintain a low supersaturation condition for heterogeneous nucleation of iron oxide, 3.5 mM H_2O_2 (Union Chemical) and 7.0 mM $FeSO_4$ (Merck) were fed continuously into the reactor bottom at 24 (± 4)°C. The pH of the solution was controlled at 3.5 to prevent $Fe(OH)_3$ precipitation. The crystals were allowed to grow on the surfaces of brick grains for 1 week. Table 1 lists the properties of the catalyst prepared from FBR. The number of fluoride-binding surface sites ($mole\,g^{-1}$) was determined following the method of Sigg and Stumm [13]. Intrinsic acidity constants (K_{a1} and K_{a2}) were obtained from graphic extrapolation of transformed acid/base titration data to zero surface charge conditions [14]. The major component coated on the catalyst surface was identified as γ-FeOOH with a Mössbauer spectrometer (Austin S-600).

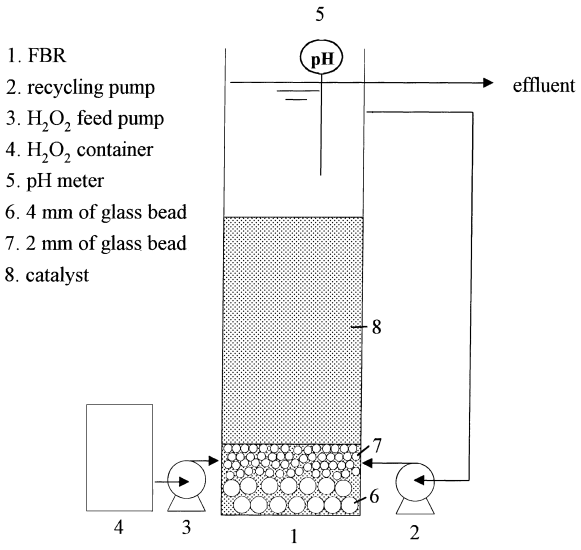

Fig. 1. The schematic diagram of the fluidized-bed reactor.

2.2. Catalytic experiments

All the catalytic experiments were conducted at room temperature (24 ± 4°C). The schematic apparatus is shown in Fig. 1. Two bench-scale FBRs were packed with 4 and 2 mm of glass beads on the bottom separately, and then the desired amount of supported γ-FeOOH catalyst grains. The smaller one (2 cm-ϕ × 100 cm-H) was applied for most of the experiments and the larger one (3 cm ϕ × 200 cm-H) was used only in part of Section 4.2. The recycle ratio of FBR was kept between 1.5 and 10 (normally above 4) except for trials studying the mixing effect. The superficial velocity was maintained at 40–60 $m\,h^{-1}$ with circulation. The applied flow rate and H_2O_2 concentration were determined from the residence time (τ) and the desired H_2O_2 dosage, respectively. To maintain a stable pH during the reaction, pH was controlled by regulating the pH of H_2O_2 feed before the experiment. The effluent was collected after 5 τs to insure that the reaction was at steady state [15]. The sample was filtered and titrated with $KMnO_4$ (Union Chemical) for the analysis of H_2O_2.

3. Theory

In the earlier literature [7,16,17], the catalytic decomposition of hydrogen peroxide with metals or metal oxides has been described by the Weiss mech-

Table 2
Mechanism proposed for decomposition of H_2O_2 on goethite [18]

$\equiv Fe^{III}OH + H_2O_2 \underset{k_{1a}}{\overset{k_1}{\Leftrightarrow}} H_2O_2\text{–}S$	(II.1)
$H_2O_2\text{–}S \underset{k_{2a}}{\overset{k_2}{\Leftrightarrow}} (\equiv Fe^{II}{}^{\bullet}O_2H) + H_2O$	(II.2)
$(\equiv Fe^{II}{}^{\bullet}O_2H) \underset{k_{3a}}{\overset{k_3}{\Leftrightarrow}} \equiv Fe^{II} + HO_2{}^{\bullet}$	(II.3)
$\equiv Fe^{II} + H_2O_2 \overset{k_4}{\rightarrow} \equiv Fe^{III}OH + {}^{\bullet}OH + H_2O$	(II.4)
$HO_2{}^{\bullet} \Leftrightarrow H^+ + O_2{}^{\bullet -}$	(II.5)
$\equiv Fe^{III}OH + HO_2{}^{\bullet}/O_2{}^{\bullet -} \rightarrow \equiv Fe^{II} + H_2O/OH^- + O_2$	(II.6)
$\equiv Fe^{II} + {}^{\bullet}OH \rightarrow \equiv Fe^{III}OH$	(II.7)

anism, in which the major reaction is:

$$H_2O_2 + S \rightarrow {}^{\bullet}OH + OH^- + S^+ \quad (1)$$

where S denotes the active site on the catalyst surface and S^+ represents the oxidized site. Recently, Lin and Gurol [18] has regarded that the Weiss mechanism cannot appropriately explain the decomposition of H_2O_2 by granular goethite. Based on the surface complexation of iron oxide, they proposed another reaction mechanism which is similar to the Fenton-like reaction of Fe^{3+}/H_2O_2 system [19]. The H_2O_2 decomposition rate (R_H) can be expressed as Eq. (2) according to the new reaction mechanism proposed in Table 2:

$$R_H = \frac{kS_T[H_2O_2]}{1 + K_H[H_2O_2]} \quad (2)$$

where $k = 2k_1k_2k_3/k'$, $K_H = k_1(k_3 + k_{2a})/k'$, $k' = k_3(k_{1a} + k_2) + k_{1a}k_{2a}$, S_T is the total concentration of the surface sites, and $[H_2O_2]$ represents the H_2O_2 concentration in the batch reactor. This equation resembles the classic Langmuir–Hinshelwood equation (L–H equation) [20] in heterogeneous catalysis, where k and K_H correspond to the rate constant and equilibrium binding constant [8]. The kinetic model has been verified at pH 7 between 1.1 and 11 mM of $[H_2O_2]$. When $K_H[H_2O_2] \ll 1$, Eq. (2) can be reduced to a second-order kinetic expression verified by Lin and Gurol [18]:

$$R_H = kS_T[H_2O_2] \quad (3)$$

4. Results and discussion

In this study, the catalytic experiments were conducted in a circulating FBR, which can be regarded as a CSTR at larger recycle ratio (R). According to the mass balance of H_2O_2 in the CSTR, the decomposition rate of H_2O_2 (R_H) can be determined directly from the inlet and outlet H_2O_2 concentrations**;** the rate is related to its conversion:

$$R_H = \frac{C_{Hi} - C_H}{\tau} = \frac{C_{Hi}X}{\tau} \quad (4)$$

where X is the conversion of H_2O_2, C_{Hi} and C_H denote the inlet and outlet H_2O_2 concentrations at steady state, respectively.

To verify the applicability of Eq. (4), the mixing effect in FBR was investigated by varying R. The result shows that R_H was independent of R at pH 7.0 ($C_{Hi} = 23.5$ mM, $\tau = 13$ min, catalyst concentration = 167 g l^{-1}). It may be due to the turbulent flow of numerous oxygen bubbles caused by higher reaction rate at pH 7.0 (as mentioned later). However, at pH 3.5 and pH 5.0, R_H remained constant when $R > 0.9$ but gradually decreased when $R < 0.9$. Since a R value of 0.9 corresponded to 15 m h^{-1} of superficial velocity under this condition, all of the following experiments were performed at $R > 1.5$ and superficial velocity > 40 m h^{-1}, which are far above these two critical values (i.e. 0.9 and 15 m h^{-1}).

4.1. Effects of H_2O_2 and catalyst concentrations

The decomposition of H_2O_2 was conducted with various inlet H_2O_2 concentrations (C_{Hi}) at pH values of 3.5, 5.0 and 7.5. The relationship between the conversion of H_2O_2 and C_{Hi} is shown in Fig. 2(a). The conversion at steady state decreases with increasing C_{Hi} at these three pH conditions. It is also found that, at the same C_{Hi}, the conversion at pH 7.5 is far larger than that at pH 3.5. To analyze the kinetics, the decomposition rate of H_2O_2 versus the outlet H_2O_2 concentrations (C_H) was plotted, as shown in Fig. 2(b). In this figure, R_H is presented as a function of outlet H_2O_2 concentration. It is shown that R_H is proportional to C_H at low H_2O_2 concentration, and the catalytic reaction is decreased with the excess H_2O_2 after reaching its maximum. Since oxygen is formed in decomposing H_2O_2, it must first be clarified whether the excess oxygen at high H_2O_2 concentration inhibits the decomposition of H_2O_2. It seems plausible that the adsorption of oxygen would compete with H_2O_2 for the active sites of the catalyst surface, thereby affect the decomposition rate of H_2O_2. The result of a control

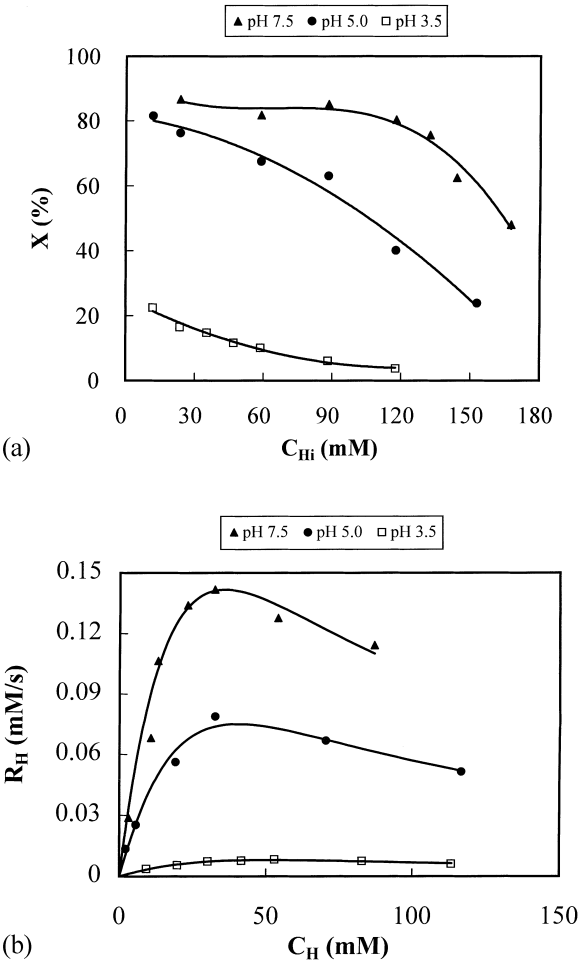

Fig. 2. Effect of H_2O_2 concentration on (a) the conversion and (b) the decomposition rate of H_2O_2. $\tau = 11.8$ min, $m = 167\ g\,l^{-1}$, m denotes the catalyst concentration.

experiment performed with introducing additional air by a small air diffuser, however, shows that increasing dissolved oxygen does not have any effect on the decomposition rate of H_2O_2. Therefore, the effect of the holdup of gaseous oxygen on the decomposition of H_2O_2 can be neglected in this reaction system.

Inhibition by excess substrate has been extensively studied in many enzymatic (bio-catalytic) systems [21,22]. Haldane [21] applied a simple model mechanism with regard to substrate inhibition:

$$\mathrm{E} + A \underset{k_{-el}}{\overset{k_{el}}{\Leftrightarrow}} EA \xrightarrow{k_{e2}} E + \text{Products} \tag{5}$$

$$\mathrm{EA} + A \underset{k_{-e3}}{\overset{k_{e3}}{\Leftrightarrow}} EA_2 \ \text{(dead-end reaction)} \tag{6}$$

where E and A denote enzyme and substrate, respectively. A commonly accepted explanation is that two substrate molecules get stuck together in the same active site (that is, we get an ineffective EA_2 complex). In high substrate concentration, the chance of forming ineffective complexes increases. Therefore, we modified the reaction mechanism proposed by Lin and Gurol (as shown in Table 2) by incorporating the substrate inhibition mechanism of enzyme kinetics [21,22]. To derive the rate equation of H_2O_2 decomposition in our reaction system, the formation of ineffective H_2O_2-catalyst surface complex (i.e., $(H_2O_2)_2-S$) is also included

$$H_2O_2\text{–}S + H_2O_2 \underset{k_{-i}}{\overset{k_i}{\Leftrightarrow}} (H_2O_2)_2\text{–}S \quad K_I = \frac{k_i}{k_{-i}} \tag{7}$$

where H_2O_2–S denotes the effective H_2O_2–catalyst surface complex, and K_I represents the equilibrium binding constant of an ineffective complex (mM^{-1}). The steady state concentration of $(H_2O_2)_2$–S can be expressed, derived from reaction (7), as:

$$\left[(H_2O_2)_2\text{–}S\right] = K_I C_H \left[H_2O_2\text{–}S\right] \tag{8}$$

The mass balance equation for the surface sites of the catalyst can be written as Eq. (9) by neglecting the species $\equiv Fe^{II}$ and $\equiv Fe^{II\bullet}O_2H$ (as shown in Table 2) due to the fact that $\equiv Fe^{II}$ is readily oxidized by H_2O_2 and $\equiv Fe^{II\bullet}O_2H$ is only a transitional state.

$$S_T = \left[\equiv Fe^{III}OH\right] + \left[H_2O_2\text{–}S\right] + \left[(H_2O_2)_2\text{–}S\right] \tag{9}$$

Therefore, R_H can be derived from a modified L–H equation (the detailed derivation is shown in the Appendix A),

$$R_H = \frac{k S_T C_H}{1 + K_H C_H (1 + K_I C_H)} \tag{10}$$

which differs from Eq. (2) only in the term $(1 + K_I C_H)$ of the denominator. Note that C_H is used here to denote the outlet H_2O_2 concentration of FBR at steady state instead of the time-variant H_2O_2 concentration in the batch reactor (i.e. $[H_2O_2]$, as indicated in Eq. (2)). Parameters in Eq. (10) can be replaced by the form used in the substrate inhibition model of enzyme kinetics [22].

$$R_H = \frac{k_H K_H C_H}{1 + K_H C_H (1 + K_I C_H)} \quad (11)$$

where $k_H = kS_T/K_H$ (mM s^{-1}). The number of the active sites on the catalyst surface is reduced by the formation of ineffective complexes, which limit the decomposition of H_2O_2. Three parameters (k_H, K_H, and K_I) in the model equation at pH values of 3.5, 5.0 and 7.5 can be determined via the linear transformation of Eq. (11), and the results are listed in Table 3.

$$\frac{C_H}{R_H} = \frac{1}{k_H K_H} + \frac{1}{k_H} C_H + \frac{K_I}{k_H} C_H^2 \quad (12)$$

It shows that k_H at pH 3.5 (e.g. 0.0355 mM s^{-1}) is much lower than those at pH 5.0 and pH 7.5 (e.g. 0.267 and 0.445 mM s^{-1}, respectively). Furthermore, K_H increases but K_I decreases with increasing pH. It is observed in Fig. 2(b) that the maxima of R_H at these pH values all occurred at 36–51 mM of H_2O_2 concentration ($C_{H,max}$), which can also be calculated using:

$$\frac{dR_H}{dC_H} = 0,\ C_{H,\,max} = \frac{1}{\sqrt{K_H K_I}} \quad (13)$$

This model seems to contradict to other observations [6,8,23,24] in which R_H follows a simple first-order relationship with respect to H_2O_2 concentration. As a matter of fact, the reaction rate with respect to $H_2O_2$was found to follow first-order at relatively low C_H in our previous study [9]. The H_2O_2 concentration that we applied in this study (i.e., 0–120 mM) was much higher than those used in other studies, therefore, inhibition on R_H at higher C_H occurred.

To simplify the kinetic behavior, we use a pseudo-first-order relationship to describe the reaction at constant catalyst amount when $C_H < C_{H,max}$. The observed first-order rate constant, k'_{obs} (s^{-1}), can be calculated from the following equation:

$$k'_{obs} = \frac{R_H}{C_H} = \frac{C_{Hi} - C_H}{C_H \tau} \quad (14)$$

Furthermore, experiments were conducted with different catalyst amounts in FBR. The result, shown in Fig. 3, demonstrates that k'_{obs} and the catalyst concentration have a good linear relationship. Therefore, we have concluded that R_H is proportional to both H_2O_2 and catalyst concentrations at low C_H, which corresponds to Eq. (3). The iron content of the catalyst surface is believed to be the key factor in catalyzing the decomposition of H_2O_2 [6,18]. We thus define k_{obs} as below, because the iron content is proportional to the catalyst concentration:

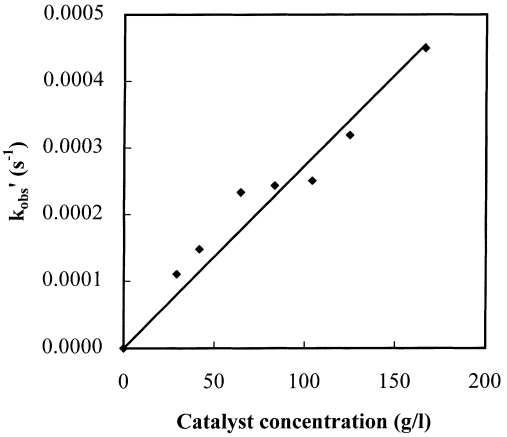

Fig. 3. Relationship between catalyst concentration and k'_{obs}. C_{Hi} = 24.4 mM, m = 167 g l^{-1}, pH = 4.8.

$$k_{obs} = \frac{k'_{obs}}{[\equiv Fe]_T} = \frac{C_{Hi} - C_H}{C_H [\equiv Fe]_T \tau} \quad (15)$$

where $[\equiv Fe]_T$ denotes the total surface concentration of iron on the catalyst per volume of FBR.

4.2. Effect of pH

According to Eq. (15), k_{obs} can be more accurately estimated by performing experiments under different τs. The change in $(C_{Hi} - C_H)/C_H/[\equiv Fe]_T$ with increasing τ at different pH conditions is depicted in Fig. 4, in which a good linear relationship between the two is shown. These slopes (k_{obs}) are listed in Table 4, showing that k_{obs} increased with increasing pH and became much larger when pH exceeded 5.5. As indicated in Table 2, $\equiv Fe^{III}OH$ was used to denote the active site of catalyst surface to simplify the reaction mechanism. As a matter of fact, the iron oxide contain three surface species: $\equiv Fe^{III}OH_2^+$, $\equiv Fe^{III}OH$ and $\equiv Fe^{III}O^-$. The equilibrium of surface chemistry [25] concerning these three species can be expressed as:

$$\equiv FeOH_2^+ \Leftrightarrow \equiv FeOH + H^+ \quad K_{a1} \quad (16)$$

$$\equiv FeOH \Leftrightarrow \equiv FeOH^- + H^+ \quad K_{a2} \quad (17)$$

Table 3
Three kinetic parameters in Eq. (11)[a]

pH	k_H (mM s^{-1})	K_H (mM^{-1})	K_I (mM^{-1})	$C_{H,max}$ (mM)	α^+	α^0	α^-
3.5	0.0355	1.16×10^{-2}	3.36×10^{-2}	51	0.984	0.016	7.82×10^{-8}
5.0	0.267	1.95×10^{-2}	3.16×10^{-2}	40	0.666	0.334	5.29×10^{-5}
7.5	0.445	2.60×10^{-2}	2.99×10^{-2}	36	0.006	0.947	0.047

[a] Calculation of α^+, α^0, and α^- is based on $pK_{a1} = 5.3$ and $pK_{a2} = 8.8$, as shown in Table 1.

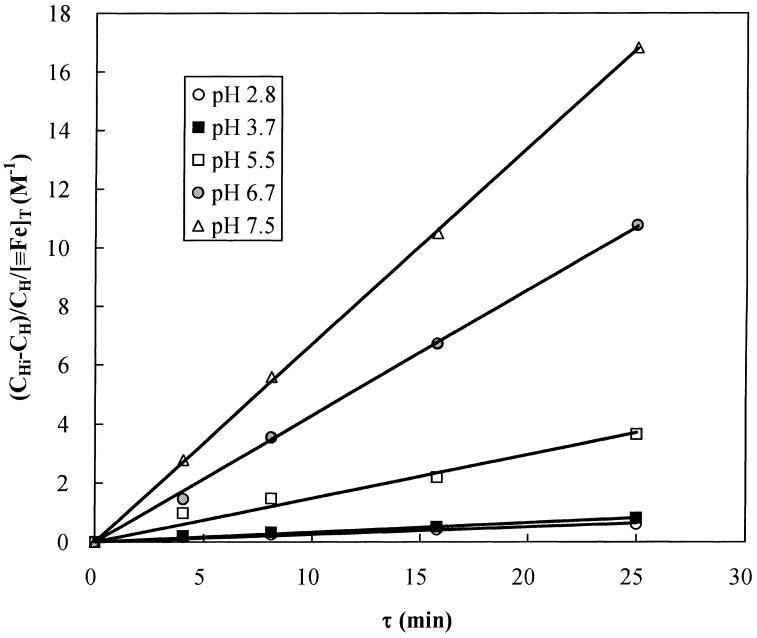

Fig. 4. Relationship between $(C_{Hi} - C_H)/C_H/[\equiv Fe]_T$ and τC_{Hi}=23.5 mM, $m = 167\ g\ l^{-1}$, $[\equiv Fe]_T = 167\ g\ l^{-1} \times 0.095$ g Fe/g catalyst = 15.9 g Fe/l = 0.283 M.

Table 4
Various k_{obs} values under different pH values

pH	k_{obs}[a] ($M^{-1}\ s^{-1}$)	pH	k_{obs}[b]
2.8	3.77×10^{-4}	2.8	2.13×10^{-4}
3.7	5.30×10^{-4}	3.5	3.87×10^{-4}
5.5	2.44×10^{-3}	5.0	2.04×10^{-3}
6.7	7.15×10^{-3}	7.0	1.01×10^{-2}
7.5	1.10×10^{-2}		

[a] Calculated from Fig. 4.
[b] Experiments were conducted in the larger FBR with 590 g l^{-1} of catalyst (C_{Hi} = 23.5 mM, τ = 33.3 min).

Thus, $[\equiv Fe^{III}OH_2^+]$ and $[\equiv Fe^{III}O^-]$ can be expressed in terms of $[\equiv Fe^{III}OH]$ without considering the electrostatic interaction, as shown in Eqs. (18) and (19)

$$\left[\equiv Fe^{III}OH_2^+\right] = \left[Fe^{III}OH\right] \times \left[H^+\right] / K_{a1} \quad (18)$$

$$\left[\equiv Fe^{III}O^-\right] = \left[\equiv Fe^{III}OH\right] \times K_{a2} / \left[H^+\right] \quad (19)$$

The variation in k_{obs} with pH may be explained by the changes in the proportion of these three different surface species. Since each species maintains a different level of binding strength with H_2O_2, according to the surface complexation theory [25,26], the binding strength between H_2O_2 and γ-FeOOH may be altered when pH is changed.

Next, experimental results were modeled using an approach similar to that of Butler and Hayes [27]. Assuming that three surface species have different reaction rates with respect to the decomposition of H_2O_2,

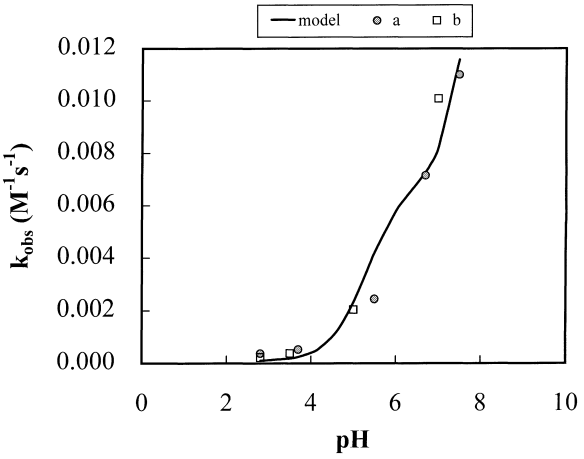

Fig. 5. Model fitting for H_2O_2 decomposition at different pH values. The experimental conditions are the same as in Table 4. The solid line represents the model prediction.

we can write the rate equation as:

$$R_H = k_{obs}\,[\equiv Fe]_T\,C_H = \left(k^+\left[\equiv Fe^{III}OH_2^+\right] + k^0\left[\equiv Fe^{III}OH\right] + k^-\left[\equiv Fe^{III}O^-\right]\right)C_H \quad (20)$$

where k^+, k^0, and k^- represent the rate constants associated with $\equiv Fe^{III}OH_2^+$, $\equiv Fe^{III}OH$, and $\equiv Fe^{III}O^-$, respectively. Eq. (20) can be transformed to:

$$k_{obs} = k^+\alpha^+ + k^0\alpha^0 + k^-\alpha^- \quad (21)$$

where $\alpha^+ = [\equiv Fe^{III}OH_2^+]/[\equiv Fe]_T$, $\alpha^0 = [\equiv Fe^{III}OH]/[\equiv Fe]_T$, and $\alpha^- = [\equiv Fe^{III}O^-]/[\equiv Fe]_T$. These three ionization fractions (α^+, α^0, α^-) of surface hydroxyl group can be calculated from Eqs. (18) and (19). The k_{obs} values in Table 4 were fitted with Eq. (21) using multiple regression of statistical techniques. Three rate constants with large differences were obtained: $k^+ = 8.67 \times 10^{-5}\,M^{-1}\,s^{-1}$, $k^0 = 6.75 \times 10^{-3}\,M^{-1}\,s^{-1}$ and $k^- = 0.109\,M^{-1}\,s^{-1}$ ($r^2 = 0.953$). To test the significance of regression, we calculated the statistic F from the analysis of variance. Since F (=40.1) $> F_{0.05,(3,5)}$ (=5.4), we conclude that α^+, α^0 and α^- contribute significantly in predicting k_{obs}. The experimental result fitted with model parameters is shown in Fig. 5, which indicates that the model agrees well with the experimental results. The change of K_R (Table 3) also demonstrates that H_2O_2 favors the sites bearing negative charge. This can be explained by the conclusion of Wallace [28]: H_2O_2 may form strong complexes with weak base sites such as $\equiv Fe^{III}O^-$.

5. Conclusions

From Section 4 we have come to the following conclusions.

1. The decomposition rate of H_2O_2 is proportional to both C_H and catalyst concentration at low C_H, but decays at high C_H, which can be interpreted using the modified Langmuir–Hinshelwood equation by incorporating the substrate inhibition model.
2. The effect of pH on k_{obs} can be attributed to the large differences in reaction rates between H_2O_2 and three surface species of iron oxide, i.e. $\equiv Fe^{III}OH_2^+$, $\equiv Fe^{III}OH$, and $\equiv Fe^{III}O^-$.

6. Notation

C_{Hi}, C_H	inlet and outlet H_2O_2 concentrations of FBR at steady state (mM)
$C_{H,max}$	outlet H_2O_2 concentration where maximum R_H occurs (mM)
$[\equiv Fe]_T$	total surface concentration of iron on the catalyst per volume of FBR (M)
S_T	total concentration of active surface sites (mM)
k	chemical reaction rate constant in Eqs. (2) and (10) ($mM\,s^{-1}$)
k^+, k^0, k^-	rate constants associated with $[\equiv Fe^{III}OH_2^+]$, $[\equiv Fe^{III}OH]$, and $[\equiv Fe^{III}O^-]$ ($M^{-1}\,s^{-1}$)
k_H	chemical reaction rate constant in Eq. (11) ($mM\,s^{-1}$)
k'_{obs}	observed first-order rate constant in decomposing H_2O_2 (Eq. (14)) (s^{-1})
$k_{obs}k'_{obs}/[\equiv Fe]_T$	($M^{-1}\,s^{-1}$)
K_I	equilibrium binding constant of an ineffective surface complex in reaction (7) (mM^{-1})
K_H	equilibrium constant in Eqs. (2), (10) and (11) (mM^{-1})
m	catalyst weight per volume of solution ($g\,l^{-1}$)
R_H	decomposition rate of H_2O_2 ($mM\,s^{-1}$)

α^+	$[\equiv Fe^{III}OH_2^+]/[\equiv Fe]_T$
α^0	$[\equiv Fe^{III}OH]/[\equiv Fe]_T$
α^-	$[\equiv Fe^{III}O^-]/[\equiv Fe]_T$
τ	residence time of FBR (min)

Acknowledgements

The authors would like to thank Dr. Y.-H. Huang of Union Chemical Laboratories, ITRI, and Dr. J.R. Pan of Chiao Tung University for their helpful discussion.

Appendix A. (detailed derivation of Eq. (10))

Since the modified mechanism incorporates the substrate inhibition model with the mechanism proposed by Lin and Gurol [18], both reaction (7) and reactions (II.1)–(II.7) (as shown in Table 2) are included in this study. The assumptions given by Lin and Gurol [18] were used in simplifying the derivation of the kinetic equations. According to the modified mechanism, the major reactions responsible for the decomposition of H_2O_2 are reactions (II.1), (7), and (II.4). The decomposition rate of H_2O_2, R_H, can be accordingly presented as:

$$R_H = k_1\left[\equiv Fe^{III}OH\right]C_H - k_{1a}\,[H_2O_2\text{–}S] + k_i\,[H_2O_2\text{–}S]\,C_H - k_{-i}\,[(H_2O_2)\,S] + k_4\left[\equiv Fe^{II}\right]C_H \quad (A.1)$$

The steady state concentration of $(H_2O_2)_2$–S can be derived from reaction (7) as:

$$k_i\,[H_2O_2\text{–}S]\,C_H = k_{-i}\left[(H_2O_2)_2\text{–}S\right] \quad (A.2)$$

Accordingly, Eq. (A.1) can be simplified to

$$R_H = k_l\left[\equiv Fe^{III}OH\right]C_H - k_{1a}\,[H_2O_2 - S] + k_4\left[\equiv Fe^{II}\right]C_H \quad (A.3)$$

The steady state concentration of H_2O_2–S can be derived from reactions (II.1), (7), and (II.2) as:

$$[H_2O_2\text{–}S] = \frac{\left(k_1\left[\equiv Fe^{III}OH\right]C_H + k_{2a}\left[\equiv Fe^{II\bullet}O_2H\right]\right)}{(k_{1a}+k_2)} \quad (A.4)$$

Since $K_I = k_i/k_{-i}$, Eq. (A.2) can be further simplified to Eq. (8). At steady state, $\equiv Fe^{II\bullet}O_2H$ is given by Eq. (A.5) based on reactions (II.2) and (II.3).

$$\left[\equiv Fe^{II\bullet}O_2H\right] = \frac{k_2\,[H_2O_2\text{–}S]}{k_3 + k_{2a}} \quad (A.5)$$

Eq. (A.4) can be transformed into Eq. (A.6) by introducing Eq. (A.5).

$$[H_2O_2 - S] = \frac{k_1\,(k_3 + k_{2a})\left[\equiv Fe^{III}OH\right]C_H}{k_3\,(k_{1a} + k_2) + k_{1a}k_{2a}} \quad (A.6)$$

From reactions (II.3) and (II.4), the $\equiv Fe^{II}$ at steady state condition is:

$$\left[\equiv Fe^{II}\right] = \frac{k_3\left[\equiv Fe^{II\bullet}O_2H\right]}{k_4 C_H} = \frac{k_3k_2\,[H_2O_2\text{–}S]}{k_4\,(k_3 + k_{2a})\,C_H} \quad (A.7)$$

Substituting Eqs. (A.6) and (A.7) into Eq. (A.3), one will obtain:

$$R_H = \frac{2k_1k_2k_3\left[\equiv Fe^{III}OH\right]C_H}{k_3\,(k_{1a} + k_2) + k_{1a}k_{2a}} \quad (A.8)$$

Since $\equiv Fe^{II}$ is oxidized rapidly by H_2O_2 and $\equiv Fe^{II\bullet}O_2H$ is only a transitional state, $[\equiv Fe^{II}]$ and $[\equiv Fe^{II\bullet}O_2H]$ are expected to be very low. The mass balance equation for the surface sites of the catalyst can be shown to be

$$\left[\equiv Fe^{III}OH\right] = S_T - [H_2O_2\text{–}S] + \left[(H_2O_2)_2\text{–}S\right] \quad (A.9)$$

Substituting Eqs. (8) and (A.6) into Eq. (A.9), one will obtain:

$$[\equiv Fe^{III}OH] = \frac{S_T}{1 + K_H C_H(1 + K_I C_H)} \quad (A.10)$$

where $K_H = k_1(k_3 + k_{2a})/k'$ and $k' = k_3(k_{1a} + k_2) + k_{1a}k_{2a}$. Finally, Eq. (A.8) can be transformed into Eq. (10) by introducing Eq. (A.10).

$$R_H = \frac{kS_TC_H}{1 + K_H C_H(1 + K_I C_H)} \quad (10)$$

where $k = 2k_1k_2k_3/k'$.

References

[1] C.P. Huang, C. Dong, Z. Tang, Waste Manage. 13 (1993) 361.
[2] S. Chou, Y.H. Huang, S.N. Lee, G.H. Huang, C. Huang, Water Res. 33 (1999) 751.

[3] R.J. Watts, A.P. Jones, P.H. Chen, A. Kenny, Water Environ. Res. 69 (1997) 269.
[4] D.L. Pardieck, E.J. Bouwer, A.T. Stone, J. Contam. Hydrol. 9 (1992) 221.
[5] C. Walling, Accounts Chem. Res. 8 (1975) 125.
[6] R.L. Valentine, H.C.A. Wang, J. Environ. Eng. 124 (1998) 31.
[7] N. Al-Hayek, M. Dore, Water Res. 24 (1990) 973.
[8] S.S. Lin, Ph.D. Dissertation, Drexel University, Philadelphia, 1997.
[9] S. Chou, C. Huang, Chemosphere 38 (1999) 2719.
[10] O. Levenspiel, Chemical Reaction Engineering, Wiley, New York, 1972.
[11] D. Kunii, O. Levenspiel, Fluidization Engineering, Wiley, New York, 1968.
[12] Y.H. Huang, G.H. Huang, S. Chou, H.S. You, S.H. Perng, A pending ROC patent 87106787, 1998.
[13] L. Sigg, W. Stumm, Colloids and Surf. 2 (1981) 101.
[14] W. Stumm, Chemistry of the Solid–Water Interface, Wiley/Interscience, New York, 1992.
[15] P.H. Calcott, Continuous Culture of Cells, vol. 1; CRC press, Boca Raton, FL, 1981, p. 21.
[16] N. Kitajima, S. Fukuzumi, Y. Ono, J. Phys. Chem. 82 (1978) 1505.
[17] P.G. Krutikov, A.V. Cheshun, V.V. Ragulin, J. Appl. Chem. USSR 57 (1984) 723.
[18] S.S. Lin, M.D. Gurol, Environ. Sci. Technol. 32 (1998) 1417.
[19] W.G. Barb, J.H. Baxendale, K.R. Hargrave, J. Chem. Soc. 121 (1950) 462.
[20] J.J. Carberry, Chemical and Catalytic Reaction Engineering, McGraw-Hill, New York, 1976.
[21] J.B.S. Haldane, Enzymes, Longmans &Green, London, 1930.
[22] J.E. Bailey, D.F. Ollis, Biochemical Engineering Fundamentals, 2nd ed., McGraw-Hill, New York, 1986, p. 115.
[23] J. Abbot, D.G. Brown, Int. J. Chem. Kinet. 22 (1990) 963.
[24] C.M. Miller, R.L. Valentine, Water Res. 29 (1995) 2353.
[25] W. Stumm, J.J. Morgan, Aquatic Chemistry, 2nd ed., Wiley/Interscience, New York, 1996.
[26] W. Stumm, B. Sulzberger, Geochim. Cosmochim. Acta 56 (1992) 3233.
[27] E.C. Butler, K.F. Hayes, Environ. Sci. Technol. 32 (1998) 1276.
[28] J.G. Wallace, Hydrogen Peroxide in Organic Chemistry, E.I. du Pont de Nemours & Co., Wilmington, Delaware, 1975.